Molecular Crystals and Liquid Crystals

Publication details, including instructions for authors and subscription information:
http://www.tandfonline.com/loi/gmcl20

Measurements of the azimuthal anchoring energy at a polyimide-nematic interface with a new transmitted light method

Sandro Faetti [a]

[a] Dipartimento di Fisica di Pisa, INFM, Pisa, Ital

Version of record first published: 18 Oct 2010

To cite this article: Sandro Faetti (2004): Measurements of the azimuthal anchoring energy at a polyimide-nematic interface with a new transmitted light method, Molecular Crystals and Liquid Crystals, 421:1, 225-234

To link to this article: http://dx.doi.org/10.1080/15421400490501842

Mol. Cryst. Liq. Cryst., Vol. 421, pp. 225–234, 2004

ISSN: 1542-1406 print/1563-5287 online
DOI: 10.1080/15421400490501842

Taylor & Francis
Taylor & Francis Group

MEASUREMENTS OF THE AZIMUTHAL ANCHORING ENERGY AT A POLYIMIDE-NEMATIC INTERFACE WITH A NEW TRANSMITTED LIGHT METHOD

Sandro Faetti
INFM and Dipartimento di Fisica di Pisa,
via Buonarroti 2,56127 Pisa, Italy

A new transmitted light method has been used to measure the azimuthal anchoring energy coefficient W at the interface between the nematic liquid crystal 5CB and a rubbed polyimide substrate. This method overcomes the typical drawbacks of the transmitted light methods and provides an unambiguous measurement of the director rotation at the surface. The contributions of the bulk director distortion are very small and can be easily separated from those due to the anchoring. The measurements can be performed also in the critical case of somewhat strong anchoring. The small optical anisotropy of the orienting layer (polyimide) can be also taken into account.

Keywords: pacs 61.30 Hn; 42.70.-a; 61.30 Gd; 78.20. Ci

1. INTRODUCTION

The classical methods used to measure the azimuthal anchoring energy consist on the optical measurement of the polarization state of either transmitted [3–13] or reflected [14–17] light. In a recent paper [18], we studied the properties of the light transmitted by a twisted NLC and we showed that a special behavior occurs for a wedged NLC cell. Exploiting these special features we proposed a new simple and accurate method to measure the azimuthal anchoring energy. This method can provide accurate measurements of azimuthal anchoring energies also in the critical case of somewhat strong azimuthal anchoring ($W > 10^{-2}$ erg/cm^2) where the classical transmitted light methods are unsuccessful [18]. In this paper, we develop this transmission light method and we measure the azimuthal anchoring

Corresponding author. Tel.: 00390502214538, Fax: 00390502214333, E-mail: Faetti@df.unipi.it

energy at the interface between the NLC 5CB and a rubbed polyimide substrate.

2. THE EXPERIMENTAL METHOD

2.1. Transmission of a Monochromatic Beam Through a Twisted Nematic Wedge

A plane electromagnetic wave of wavelength λ propagates along the z-axis, passes through a polarizer which rotates with the angular frequency ω, and impinges normally on a nematic sample contained between two optically isotropic plates making a small wedge angle ($\theta \sim 1^\circ$) as shown schematically in Figure 1. A uniform magnetic field $\boldsymbol{H}$ can be applied along the x-axis and the director field lies everywhere in the layer plane x-y (the small wedge angle can be disregarded). The incident beam is separated by the nematic wedge into a generalized extraordinary beam and a generalized ordinary beam [18]. We define the small parameter.

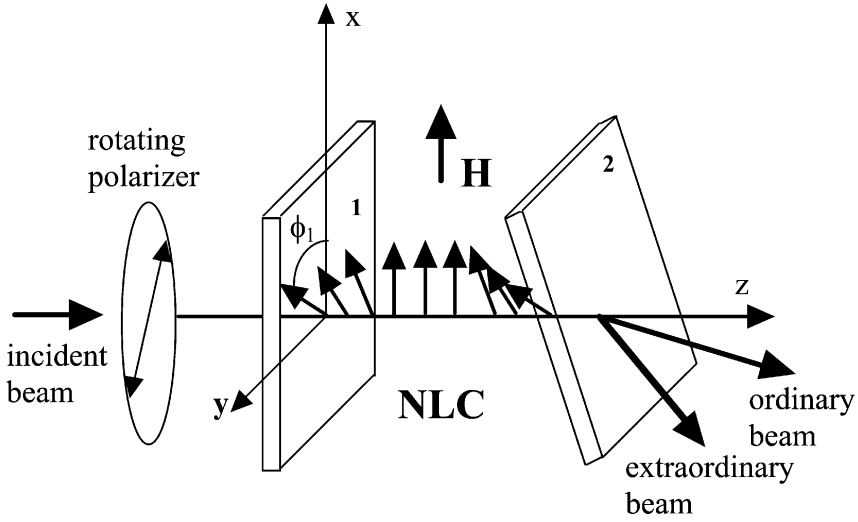

FIGURE 1 A nematic liquid crystal (NLC) is enclosed between two solid plates that make a wedge with a small angle $\sim 1^\circ$. A polarized laser beam passes through a rotating polarizer and impinges at normal incidence on plate 1. The laser beam is separated into an ordinary and an extraordinary beam. The wedge angle and the refraction angles have been exaggerated in order to make the figure clearer. The arrows in the region between the plates represent the local directors. ϕ_1 is the azimuthal angle of the director at surface 1.

$$\alpha = \frac{\lambda}{2\pi\Delta n\xi}, \tag{1}$$

where ξ is the magnetic coherence length

$$\xi = \sqrt{\frac{K_{22}}{\chi_a}}\frac{1}{H}. \tag{2}$$

$\Delta n = n_e - n_o$ is the anisotropy of the refractive indices of the NLC, K_{22} is the twist elastic constant, χ_a is the anisotropy of the magnetic susceptibility. α is proportional to H with $\alpha \approx 0.14$ for a 5CB sample at temperature T = 25°C and $H = 5$ kOe. Using the Berreman theory [19], we find that the intensity of the output extraordinary beam is [18]:

$$I_e^{out} = I_A + I_B \cos 2(\omega t - \phi_1 - \gamma), \tag{3}$$

where I_A, I_B and γ are coefficients and the polarizer is assumed to be parallel to the magnetic field at time $t = 0$. This intensity is characterized by angular frequency 2ω and phase coefficient

$$\beta = 2(\phi_1 + \gamma). \tag{4}$$

γ is a coefficient of the second order in α and can be disregarded in many practical cases. In this case, we find $\phi_1 = \beta/2$ which corresponds to the prediction of the adiabatic theorem [5–7]. Note that, in the standard geometry with nematic planar layers, the corrections to the adiabatic theorem are much greater because they are usually of the first order in α [5,18]. Coefficient γ in Eq. (4) is equivalent to a small apparent rotation $\Delta\phi = \gamma$ of the director at surface 1 and depends greatly on angle ϕ_1 at surface 1, but is nearly independent of angle ϕ_2 at surface 2. Here, we consider a cell having the same orientations of the easy axes on the two interfaces and the same anchoring energies. Then, $\phi_1 = \phi_2$ for each amplitude of the magnetic field. Figure 2 shows γ versus the square power of α for different values of ϕ_1 and for the nematic 5CB at temperature $T = 25$°C. The maximum value $\alpha^2 = 0.078$ in Figure 2 corresponds to $H = 10$ kOe. We emphasize that: 1) γ is nearly proportional to α^2; 2) $\gamma \approx 0$ for $\phi_1 = 0^\circ$ or $\phi_1 = 90^\circ$. In particular:

$$\gamma = c_o\alpha^2 \sin 2\phi_1 + O(\alpha^4) = b_o H^2 \sin 2\phi_1 + O(H^4), \tag{5}$$

where c_o depends only on the optical parameters of the NLC [20] and of the substrate and $O(\alpha^4)$ is a contribution of order α^4. Then, the choice $\phi_e \approx 90^\circ$ extends enormously the range of validity of the simple adiabatic result $\phi_1 = \beta/2$. Let's consider, for instance, a 5CB sample at $T = 25$°C with $\phi_1 = 89^\circ$ which is subjected to the magnetic field $H = 5$ kOe. With the

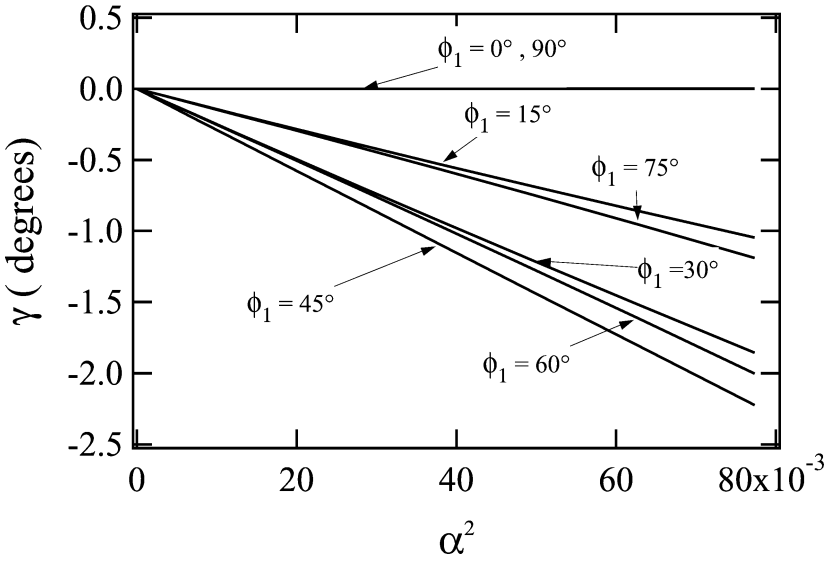

FIGURE 2 Apparent surface rotation angle γ versus the square power of α for different values of angle ϕ_1 at the first interface ($\phi_1 = \phi_2$). The material parameters used to make the calculations are those of 5CB at $T = 25^{\circ}C$: $n_e = 1.717$, $n_o = 1.528$ [20], $K_{22} = 3.93\ 10^{-7}$ dynes [21], $\chi_a = 1.07\ 10^{-7}$ (c.g.s. unities) [22]. The refractive index of the substrate is $n_s = 1.51$.

standard planar nematic layers (see, for instance, refs. [5] and [18]), the apparent surface rotation can reach $\gamma \sim 6^{\circ}$, while it is reduced to $\gamma \sim 0.02^{\circ}$ with the present method.

2.2. The Experimental Procedure to Measure the Anchoring Energy Coefficient

Here we assume that the local thickness d of the nematic sample is much greater than ξ and that $\Delta\phi_1(H) = \phi_1(H) - \phi_e$ is small enough. In these conditions, we obtain [1,2]:

$$\Delta\phi_1 = -\frac{\sqrt{K_{22}\chi_a}}{W} H \sin\phi_e, \tag{6}$$

where W is the azimuthal anchoring energy coefficient [1,2] and where we have exploited the condition $\phi_1 = \phi_e + \Delta\phi_1 \cong \phi_e$. From Eq. (4) we get

$$\Delta\phi_1(H) = \frac{\Delta\beta(H)}{2} - \gamma(H), \tag{7}$$

If γ is negligible, $\Delta\phi_1 = \Delta\beta/2$ and W can be simply obtained from the measurement of the proportionality coefficient between $\Delta\beta$ and H (see Eq. (6)). Note that $\gamma(H)$ is a quadratic function of H (Eqs. (1) and (2) and Fig. 2). Therefore, the correctness of the proposed procedure can be controlled looking at the linearity of $\Delta\beta$ on H.

So far we assumed that the NLC is sandwiched between two optically isotropic plates. However, in the case of the standard polymeric layers (polyimide, PVA), the rubbing procedure induces an alignment of the polymeric chains [23] and a consequent optical anisotropy. The optical axis is parallel to the rubbing direction. Dephasing δ_p between the extraordinary and ordinary rays is an increasing function of the rubbing strength [23] (typically $\delta_p < 1^\circ$). Similar dephasings were measured in the case of photosensitive polymeric films irradiated by linearly polarized UV light [24]. The anisotropy of the aligning layer leads to a very small further apparent surface rotation γ^*. For $\delta_{\rm p} \ll 1$ rad, using the Oldano perturbative approach [5–7] and neglecting the reflections from the various interfaces and the contributions of the second order in α we get

$$\gamma^* = \eta_1 \sqrt{\frac{n_o}{n_e}} \alpha \sin\phi_e = \eta_1 \frac{1}{\Delta k} \sqrt{\frac{n_o \chi_a}{n_e K_{22}}} \delta_p H \sin\phi_e, \tag{8}$$

where $\eta_1 = \left[\sqrt{n_e/n_o} + \sqrt{n_o/n_e}\right]/2 \approx 1$, $\Delta\kappa = 2\pi(n_{\rm e} - n_o)/\lambda$ and n_e and n_o are the extraordinary and ordinary refractive indices of the NLC. This contribution is usually negligible except for strong anchoring ($\gamma^* < 0.14^\circ$ for 5CB with $T = 25^\circ$C, $H = 5$ kOe and $\delta_p < 1^\circ$).

3. EXPERIMENT

In order to prove the ability of the proposed method to measure somewhat strong azimuthal anchoring energies, we used a strongly rubbed polyimide film as orienting medium. The polyimide coated plates were purchased from EHC Ltd. The glass plates (refractive index $n_s = 1.51$) are covered by a 200 Å thin film of indium-tin oxide and by a thin hardly rubbed polyimide layer [Hitachi Chemical LX-5400(PIX-1400)]. The polyimide layer is rubbed using a polyester roll. The rubbing parameters are: polyester fiber length = 8 mm; diameter = 58 mm; roll rotation speed = 600 rpm; speed of glass = 2 m/min and number of times = 7. This rubbing procedure ensures a strong enough azimuthal anchoring with a pretilt angle lower than 1°. The optical dephasing introduced by the thin polyimide film has been measured using the Senarmont method [25]. We find $\delta_{\rm p} = 0.1^\circ \pm 0.02^\circ$. This dephasing produces a maximum spurious rotation $\gamma^* \approx 0.02^\circ$ at the maximum applied magnetic field $H = 7.76$ kOe [see Eq. (8)]. This spurious rotation is smaller than the random noise which is present in our experiment

($\approx \pm 0.05^\circ$) and, thus, it will be disregarded in the analysis of the experimental results. A wedge cell ($\theta \sim 1^\circ$) is built using two identical plates separated by two mylar spacers of different thickness (60 μm and 160 μm). The nematic LC 4-pentyl-4′-cyanobiphenil (5CB) is purchased from MERK and has the clearing temperature $T_{NI} = 35^\circ$C. 5CB is introduced by capillarity between the glass plates in its isotropic phase in order to avoid possible aligning effects of the liquid flow [26]. A schematic view of the experimental set-up is shown in Figure 3. The cell is contained in a thermostat which ensures a stability better than 0.02°C and lies between the polar expansions of a Brucker electromagnet. A He-Ne laser beam ($\lambda = 632.8$ nm and diameter ≈ 1 mm) passes through a rotating polarizer P and impinges at normal incidence on the first glass plate of the cell. The extraordinary beam impinges on photodiode Ph_1, while the ordinary beam is stopped by a black screen (BS). A part of the incident beam is reflected (at nearly normal incidence) by the glass plate G, passes through the analyzer A and is collected by photodiode Ph_2. Polarizer P rotates with the constant angular velocity $\omega = 1.88$ rad/s. In these conditions, the outputs $I_1(t)$ and $I_2(t)$ of photodiodes Ph_1 and Ph_2 are sinusoidal functions of time t with pulsation 2ω. A PC performs the Fourier analysis of them at frequency 2ν and calculates amplitudes A_1 and A_2 and phases β_1 and β_2. Signal $I_2(t)$ gives a reference for the phase and the phase difference $\beta = \beta_1 - \beta_2$ is measured. When the magnetic field is switched on, the change $\Delta\beta$ of the phase difference between the two signals is measured. The surface director rotation $\Delta\phi_1$ is related to the measured phase change $\Delta\beta$ by Eq. (7).

In our standard experimental conditions, we set $\phi_e = 85^\circ \pm 1^\circ$. To measure the azimuthal anchoring energy, we switch on a magnetic field of amplitude H and we measure the corresponding phase variation $\Delta\beta$ after a few seconds when the director field has reached its stationary value. For this kind of substrates we find that the gliding [27] of the easy axis

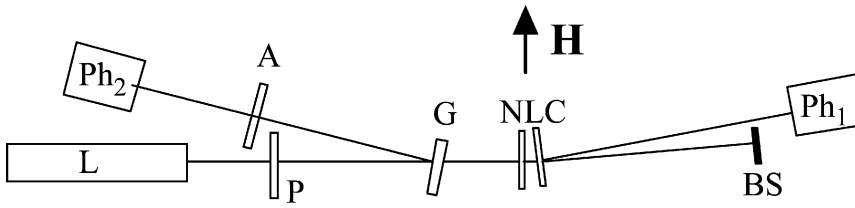

FIGURE 3 Schematic view of the experimental apparatus used to measure the azimuthal anchoring energy. L = He-Ne Laser, P = rotating polarizer, A = analyzer, NLC = nematic wedge cell, G = glass plate, Ph_1 and Ph_2 = photodiodes, BS = black screen, H = magnetic field. All the angles are exaggerated in order to make the figure clearer.

is negligible during this short time. The main uncertainty in the measurement of the phase change $\Delta\beta$ comes from the phase noise that is of the order of $\pm\,0.1^\circ$ and leads to an uncertainty of $\pm\,0.05^\circ$ on the surface director rotation angle $\Delta\phi_1 \approx \Delta\beta/2$ (Eq. (7)). Full points in Figure 4 represent $-\Delta\beta/2$ versus the magnetic field amplitude H for $T = 25^\circ$C and $\phi_e = 85^\circ \pm 1^\circ$. In agreement with the theory, $-\Delta\beta/2$ is a linear function of H for small enough magnetic fields (see Eq. (6)) but non-linear contributions are clearly visible for $H > 2$ kOe. They are due to the non-adiabatic contribution γ in Eq. (7). The full straight line represents the best fit of the experimental results below $H = 2$ kOe with the linear function $-\Delta\beta/2 = a_1\,H$, where a_1 is a free coefficient (the best fit value is $a_1 = 1.03\ 10^{-4}$ deg/Oe). The azimuthal anchoring energy coefficient is calculated using the expression:

$$W = \frac{\sqrt{K_{22}\chi_a}}{a_1}\sin\phi_e. \tag{9}$$

Using $K_{22} = 3.93\ 10^{-7}$ dynes [21], $\chi_a = 1.07\ 10^{-7}$ [22], $\phi_e = 85^\circ$ and $a_1 = 1.8\ 10^{-6}$ rad/Oe we get $W = (1.13 \pm 0.2)\ 10^{-1}$ erg/cm^2 which is a relatively strong azimuthal anchoring energy (it corresponds to an extrapolation

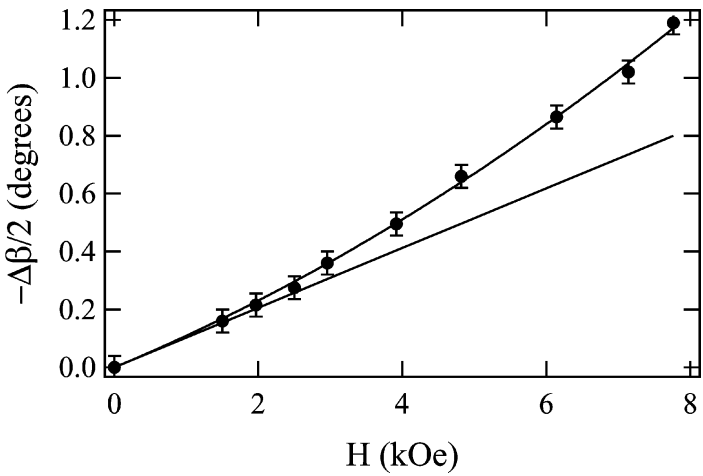

FIGURE 4 $\Delta\beta/2$ versus the intensity of the magnetic field when the easy director angle at surface 1 is $\phi_e = 85^\circ \pm 1^\circ$ and temperature is T = 25°C. Points represent the experimental results, the full straight line represents the best fit of the experimental results obtained for H < 2 kOe with the linear function $-\Delta\beta/2 = a_1\,H$. The full curve represents the best fit of the experimental points with function $-\Delta\beta/2 = a_1 H + a_2 H^2$.

length $\beta = K_{22}/W = 34.8\,\text{nm}$). The experimental results in the whole range of magnetic fields are well represented by the quadratic function:

$$-\frac{\Delta\beta}{2} = a_1 H + a_2 H^2, \tag{10}$$

where the linear contribution is the true surface rotation angle $\Delta\phi_1$, while the quadratic contribution is due to the non-adiabatic apparent rotation γ (see Eqs. (5) and (7)). The full curved line in Figure 4 represents the best fit of the experimental results with the quadratic function in Equation (10).

Figure 5 shows $-\Delta\beta/2$ versus intensity H of the magnetic field for $\phi_e = 43.3^\circ$. Now, according to Eq. (5), the apparent rotation γ gives a much more important contribution to the experimental results. The straight line in Figure 5 represents the theoretical dependence of $-\Delta\beta/2$ which is obtained disregarding the non-adiabatic contributions [$\gamma = 0$ in Eq. (7)] and substituting the measured anchoring energy coefficient $W = 1.13\ 10^{-1}$ erg/cm^2 in Equation (6). The full curve in Figure 5 corresponds to the best fit of the experimental results with Equation (10). According to the theory [see Eq. (5)], a_2 is expected to be proportional to $\sin(2\phi_1) \sim \sin(2\phi_e)$. Full points in Figure 6 show coefficient a_2 versus angle ϕ_e, while the full curve represents the best fit of the

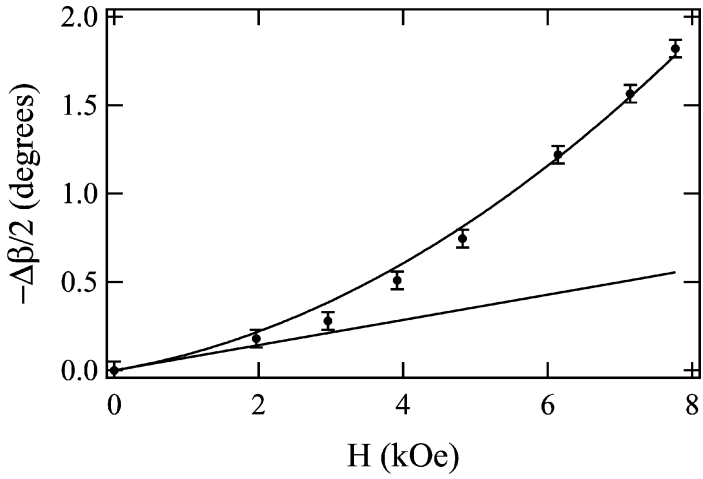

FIGURE 5 $\Delta\beta/2$ versus the intensity of the magnetic field when the easy director angle at surface 1 is $\phi_e = 43.3^\circ \pm 1^\circ$ and temperature is T=25°C. Points represent the experimental results, the broken straight line represents the behavior which is predicted in the absence of non-adiabatic contributions (γ=0). The full line is the best fit with Equation (10).

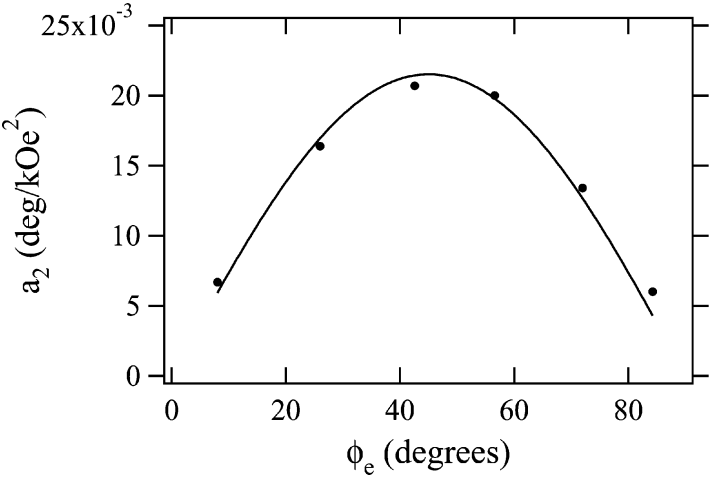

FIGURE 6 Coefficient a_2 in Equation (10) versus the easy azimuthal angle ϕ_e. The full line represents the best fit with function $a_2 = b_o \sin 2\phi_e$ (see Eq. (5)).

experimental data with function $a_2 = b_o \sin(2\phi_e)$ [see Eq. (5)]. From the best fit we obtain $b_o = 0.0215 \pm 0.001\,\text{deg/kOe}^2$ which is in a satisfactory agreement with the value $b_o = 0.0224\,\text{deg/kOe}^2$ which is calculated using the numerical integration of the Berreman equations with $n_e = 1.717$ and $n_o = 1.528$ [20], $K_{22} = 3.93\ 10^{-7}$ dynes [21] and $\chi_a = 1.07\ 10^{-7}$ (c.g.s. unities) [22].

4. CONCLUSIONS

A new transmitted light method has been developed based on the theoretical predictions of the Berreman optical theory. This method uses a nematic twisted wedge and improves greatly the accuracy and the measurement range of the conventional light transmission methods. Accurate measurements of somewhat strong azimuthal anchoring energies are possible with this method. All the qualitative and quantitative theoretical predictions have been confirmed by our experimental results. In particular, the main corrections to the adiabatic theorem are quadratic in the intensity of the magnetic field and become very small if the surface director is nearly orthogonal to the magnetic field. The measurement method and the analysis of the experimental results is very simple and direct. Furthermore the contributions due to the bulk director distortion can be easily distinguished from the anchoring ones simply looking at the linearity of the dependence of $\Delta\beta$ on H.

REFERENCES

[1] de Gennes, P. G. (1974). *The physics of liquid crystals*, Oxford: Clarendon.
[2] Faetti, S. (1991). *Physics of Liquid Crystalline Materials*, Khoo, I. C. & Simoni, F. (Eds.), Gordon and Breach Science Publishers.
[3] Sicart, J. (1976). *J. Physique Lett.*, *37*, L-25.
[4] van Sprang, H. A. (1983). *J. Physique (Paris)*, *44*, 421.
[5] Barbero, G., Miraldi, E., Oldano, C., Rastrello, M. L., & Valabrega, P. T. (1986). *J. Physique (Paris)*, *4*, 1411.
[6] Allia, P., Oldano, C., & Trossi, T. (1987). *Mol. Cryst. Liq.Cryst.*, *143*, 17.
[7] Allia, P., Oldano, C., & Trossi, T. (1988). *Phys. Scr.*, *37*, 755.
[8] Oh Ide, T., Kuniyasu, S., & Kobayashi, S. (1988). *Mol. Cryst. Liq. Cryst.*, *164*, 91.
[9] Faetti, S. & Lazzari, C. (1992). *J. Appl. Phys.*, *71*, 3204.
[10] Polossat, E. & Dozov, I. (1996). *Mol. Cryst. Liq. Cryst.*, *282*, 223.
[11] Adrienko, D., Dyadyusha, A., Iljin, A., Kurioz, Yu., & Reznikov, Yu. (1998). *Mol. Cryst. Liq. Cryst.*, *321*, 271.
[12] Vorflusev, V., Kitezerow, H., & Chigrinov, V. (1995). *Jpn. J. Appl. Phys.*, *34*, L1137.
[13] Akahane, T., Kaneko, H., & Kimura, M. (1996). *Jpn. J. Appl. Phys.*, *35*, 4434.
[14] Faetti, S. & Mutinati, G. C. (2003). *Eur. Phys.*, *J. E 10*, 265.
[15] Faetti, S., Palleschi, V., & Schirone, A. (1988). *Il Nuovo Cimento*, *10D*, 1313.
[16] Faetti, S., Nobili, M., & Schirone, A. (1991). *Liq. Cryst.*, *10*, 95.
[17] Faetti, S. & Nobili, M. (1998). *Liq. Cryst.*, *25*, 487.
[18] Faetti, S. & Mutinati, G. C. *Phys. Rev. E*, in press.
[19] Berreman, D. W. (1972). *J. Opt. Soc. Am.*, *62*, 502.
[20] Karat, P. P. & Madhusudana, N. V. (1976). *Mol. Cryst. Liq. Cryst.*, *36*, 51.
[21] Toyooka, T., Chen, G., Takezoe, H., & Fukuda, A. (1987). *Jpn. J. Appl. Phys.*, *26*, 1959.
[22] Scherrel, P. L. & Crellin, D. A. (1979). *J. Physique Colloq.*, *40*, C3-213.
[23] van Aerle, N. A. J. M., Barmentlo, M., & J. Hallering, R. W. (1993). *J. Appl. Phys.*, *74*, 3111.
[24] Bryan-Brown, G. P. & Sage, I. C. (1996). *Liq. Cryst.*, *20*, 285.
[25] Bruhat, G. *Cours de Physique Générale: Optique*, (Masson & C^{ie} Editions, Paris)
[26] Yokoyama, H., Kobayashi, S., & Kamei, H. (1984). *J. Appl. Phys.*, *56*, 2645.
[27] Faetti, S., Nobili, M., & Raggi, I. (1999). *Eur. Phys. J. B*, *11*, 445.